A Comparative Study of Nature-Inspired Optimization Techniques for MLP-Based Sentinel-2 Image Segmentation

Abdullah Furkan Yeğin [1]*, İsmail Rakıp Karaş[1], Sohaib K M Abujayyab[2]

[1] Department of Computer Engineering, Karabuk University, Demir Celik Campus, 78050 Karabuk, Turkey - abdullahfurkanyegin@outlook.com, ismail.karas@karabuk.edu.tr
[2] Dept. of Geography, Karabuk University, Demir Celik Campus, 78050 Karabuk, Turkey - sjayyab@karabuk.edu.tr

Keywords: Sentinel-2, land cover classification, MLP, nature-inspired optimization, remote sensing, machine learning

Abstract

Accurate land cover classification using Sentinel-2 satellite imagery remains a critical challenge in remote sensing due to spectral complexity and spatial heterogeneity. This study presents a comprehensive evaluation of Multi-Layer Perceptron (MLP) models optimized with nature-inspired algorithms for Sentinel-2 image segmentation. We compare five optimization approaches Ant Colony Optimization (ACO), Whale Optimization Algorithm (WOA), Particle Swarm Optimization (PSO), Genetic Algorithm (GA), and Artificial Bee Colony (ABC) to enhance MLP performance for classifying five key land cover types: urban areas, agricultural fields, sparse vegetation, water bodies, and forests. Our optimized MLP architecture achieves superior performance with 90.8% overall accuracy, 90.7% F1-score, 0.883 Cohen's Kappa, and 0.981 ROC-AUC, representing a 7.2% improvement over the best-performing nature-inspired algorithm (GA/WOA at 83.6% accuracy). Class-specific analysis reveals high accuracy for water bodies (94.2% F1-score) and forests (91.6%), while urban areas (87.4%) and sparse vegetation (82.7%) present greater challenges due to spectral similarities. The study demonstrates that hybrid optimization, combining algorithmic tuning with expert refinement, yields the most robust results for operational land cover mapping. Key findings highlight GA's effectiveness in handling class imbalance and WOA's strength in rare class detection. Computational efficiency (2–4 hours training time) further supports the model's feasibility for large-scale applications. This research advances Sentinel-2 segmentation methodologies while providing practical insights for environmental monitoring, precision agriculture, and urban planning.

1. Introduction

Remote sensing technologies have revolutionized our ability to monitor and analyze Earth's surface dynamics, providing unprecedented opportunities for environmental monitoring, urban planning, and natural resource management (Phiri et al., 2020). Among the various satellite systems available today, the Sentinel-2 mission, launched as part of the European Union's Copernicus program, has emerged as a cornerstone for land cover classification and change detection due to its unique combination of spatial, spectral, and temporal resolution (Phiri and Morgenroth, 2017). With its 13 spectral bands covering wavelengths from visible to shortwave infrared (SWIR) and a revisit time of 5 days at the equator, Sentinel-2 provides researchers and practitioners with a powerful tool for systematic Earth observation (Karaboga and Basturk, 2007). The mission's open data policy has further democratized access to high-quality satellite imagery, enabling widespread applications in precision agriculture, forestry, water resource management, and disaster monitoring (Dorigo et al., 2006).

Despite these advancements, accurate segmentation of Sentinel-2 imagery remains a significant challenge in remote sensing research (Mirjalili and Lewis, 2016). The complexity arises from several factors: (1) spectral similarity between different land cover classes, particularly in agricultural and natural vegetation areas (Kennedy and Eberhart, 1995); (2) atmospheric effects and cloud contamination that degrade image quality (Holland, 1992); (3) seasonal variations in vegetation phenology that alter spectral signatures (Gascon et al., 2017); and (4) the high dimensionality of multispectral data that increases computational demands (Cheng et al., 2017). Traditional image segmentation approaches, including thresholding methods, region-growing algorithms, and unsupervised clustering techniques, often struggle to achieve satisfactory accuracy when dealing with these challenges (Wulder et al., 2016). While these methods are computationally efficient, they typically fail to capture the complex, non-linear relationships present in multispectral satellite data (McHugh, 2012).

The advent of machine learning techniques has brought new opportunities for addressing these challenges in satellite image analysis (Giuliani et al., 2018). Among various machine learning approaches, Multi-Layer Perceptron (MLP) networks have demonstrated promise for remote sensing applications due to their ability to model complex spectral relationships through hierarchical feature learning (Defourny et al., 2019). MLPs can effectively capture the non-linear interactions between different spectral bands, making them well-suited for land cover classification tasks (Hansen et al., 2013). However, the performance of MLP models is highly dependent on proper architecture design and hyperparameter selection, including the number of hidden layers, neuron configuration, activation functions, and regularization parameters (Maxwell et al., 2018). Suboptimal choices in these parameters can lead to poor generalization, overfitting, or slow convergence during training (Gómez et al., 2016).

Recent advances in optimization algorithms have opened new possibilities for enhancing the performance of machine learning models in remote sensing applications (Çiçekli, 2022). Nature-inspired optimization techniques, including Ant Colony Optimization (ACO), Whale Optimization Algorithm (WOA), Particle Swarm Optimization (PSO), Genetic Algorithm (GA), and Artificial Bee Colony (ABC), have shown promise for solving complex optimization problems in machine learning (Durmazbilek, 2021). These algorithms mimic natural processes such as biological evolution, swarm intelligence, and animal foraging behavior to efficiently explore high-dimensional parameter spaces (Seto et al., 2012). When applied to MLP hyperparameter tuning, these methods can potentially overcome the limitations of manual parameter selection and grid search

approaches, which are often time-consuming and computationally expensive (Esch et al., 2013). Several studies have demonstrated the effectiveness of these optimization techniques in improving the performance of machine learning models for various remote sensing applications (Pesaresi et al., 2013).

This study aims to advance the field of satellite image segmentation by conducting a comprehensive evaluation of optimized MLP models for Sentinel-2 land cover classification. Our research focuses on five key land cover classes: urban areas, agricultural fields, sparse vegetation, water bodies, and forests. We employ nine carefully selected Sentinel-2 spectral bands that capture distinct features of these land cover types, including the visible spectrum for basic land-water discrimination, red-edge bands for vegetation stress detection, and SWIR bands for soil moisture and mineral content analysis (Yalçın, 2022). The study systematically compares the performance of five nature-inspired optimization algorithms (ACO, WOA, PSO, GA, and ABC) in tuning MLP hyperparameters, with particular attention to their ability to improve classification accuracy while maintaining computational efficiency.

The significance of this research extends beyond methodological advancements in image segmentation. Accurate land cover classification from Sentinel-2 imagery has important practical implications for numerous applications. In agriculture, it enables precision farming practices and yield prediction (Alonso et al., 2013). In forestry, it supports sustainable management and carbon stock estimation (Defourny et al., 2019). For urban areas, it facilitates growth monitoring and infrastructure planning (Dronova, 2015). Moreover, the integration of optimized machine learning models into operational Earth observation systems can enhance our ability to monitor and respond to environmental changes at global scales (Li et al., 2020).

2. Methodology

2.1 Study Area and Dataset Description

The study area encompasses a 3,670 km² region centered on Ankara, Turkey (39.93° N, 32.85° E), selected for its diverse land cover characteristics (McFeeters, 1996) (See Figure 1). This geographical location presents a complex mosaic of urban landscapes, agricultural zones, forested areas, and water bodies, making it an ideal testbed for evaluating land cover classification algorithms. The region experiences distinct seasonal variations in vegetation phenology, with average annual precipitation of 400 mm and temperatures ranging from −5 °C in winter to 30 °C in summer (Rouse et al., 1974). These climatic conditions create dynamic spectral signatures across different land cover types throughout the year, posing significant challenges for accurate image segmentation.

For this research, we utilized Sentinel-2 Level-2A (L2A) surface reflectance products acquired on May 11, 2021, corresponding to the peak vegetation growth period in the region (Lu and Weng, 2007). The dataset was obtained from the Copernicus Open Access Hub. May imagery was specifically selected to capture optimal vegetation conditions while minimizing cloud interference, which typically increases during summer months in the study area (Otsu, 1979). The Level-2A processing includes atmospheric correction using the Sen2Cor algorithm, providing bottom-of-atmosphere reflectance values essential for accurate land cover classification (Sankur, 2004).

Figure.1. Geographic location and boundaries of the study area (Ankara, Turkey).

The ground truth dataset consists of 3,000 carefully annotated samples (600 per land cover class), distributed proportionally across the study area to ensure representative coverage. Sample collection followed a stratified random sampling approach, with reference data derived from multiple sources: (1) high-resolution (0.5 m) aerial orthophotos from the Turkish National Mapping Agency, (2) field surveys conducted during the satellite overpass period, and (3) ancillary data from the CORINE Land Cover inventory (Pham et al., 2000).

Five distinct land cover classes were identified and validated by domain experts: Urban/Built-up Areas: Including residential, commercial, and industrial zones with characteristic high reflectance in visible and SWIR bands (Canny, 1986). Agricultural Land: Predominantly cultivated fields with seasonal crops exhibiting unique phenological patterns. Sparse Vegetation: Grasslands and shrublands with intermittent vegetation cover. Water Bodies: Natural and artificial water features including rivers, lakes, and reservoirs. Dense Forest: Deciduous and coniferous woodlands with continuous canopy cover.

The spatial distribution of samples was carefully designed to account for edge effects and transitional zones between land cover types, with a minimum buffer distance of 100 m maintained between samples to ensure spatial independence (Blaschke et al., 2014). Each sample corresponds to a 20 × 20 pixel window (400 m² at 20 m resolution) to capture sufficient spatial context while maintaining class purity. The dataset was divided into training (70%), validation (15%), and test (15%) sets using a stratified random split to preserve class distribution across all subsets (Jain, 2010). This comprehensive dataset preparation ensures robust model training and evaluation while minimizing potential biases in the classification process.

2.2 Model Architectures

This study implements and compares multiple machine learning approaches for Sentinel-2 image segmentation, with particular emphasis on optimized neural network architectures. The selected models were specifically designed to address the unique challenges of multispectral satellite image classification, including high-dimensional spectral data, class imbalance, and spatial heterogeneity, while maintaining computational efficiency suitable for large-scale operational applications. Our architectural design philosophy prioritizes both classification accuracy and model interpretability, ensuring practical utility for remote sensing applications.

The foundation of our approach employs a Multi-Layer Perceptron (MLP) implemented using scikit-learn's MLPClassifier. The base architecture features an input layer with 9 nodes corresponding to the carefully selected Sentinel-2 spectral bands (B2, B3, B4, B5, B6, B7, B8, B11, B12). Three hidden layers with 199 neurons utilize Rectified Linear Unit (ReLU) activation functions to model the complex non-linear relationships between spectral bands. The output layer consists of 5 nodes with softmax activation, representing our target land cover classes: urban areas, agricultural land, sparse vegetation, water bodies, and dense forest. To enhance generalization and prevent overfitting, we incorporate several regularization techniques including L2 penalty (α=0.97), inter-layer dropout (rate=0.3), batch normalization between hidden layers, and early stopping with a patience of 10 epochs. The model is trained using the Adam optimizer with an initial learning rate of 0.001 and batch size of 32 samples, configurations determined through extensive preliminary experiments to establish a robust performance baseline.

Building upon this foundation, we systematically enhanced the base MLP through hyperparameter optimization using five nature-inspired algorithms, each selected for their complementary strengths in navigating complex parameter spaces. The Ant Colony Optimization (ACO)-MLP variant incorporates pheromone-based feature weighting and optimizes the hidden layer configuration to 256-128-64 neurons with layer-specific dropout rates (0.4 → 0.2). The Whale Optimization Algorithm (WOA)-MLP implements dynamic neuron allocation through its distinctive bubble-net inspired search mechanism and encircling prey approach for adaptive learning rate adjustment. Particle Swarm Optimization (PSO)-MLP utilizes swarm intelligence for weight initialization and velocity-controlled layer size optimization, while the Genetic Algorithm (GA)-MLP employs chromosomal encoding of network topology with tournament selection and single-point crossover operations. The Artificial Bee Colony (ABC)-MLP completes our ensemble with its unique employed bee phase for local search, onlooker bee phase for global exploration, and scout bee phase for architectural innovation. Each optimization algorithm was configured with a population size of 50 and executed for 100 iterations, with performance evaluated using rigorous 5-fold cross-validation on the training set to ensure robust parameter selection.

2.3 Accuracy evaluation

To comprehensively assess the segmentation performance, we employed seven robust evaluation metrics measuring different aspects of classification accuracy. The Overall Accuracy (OA) provided a global measure of correct classifications. For class-specific evaluation, we computed Precision to measure prediction reliability and Recall to assess detection capability, combining them in the F1-Score (harmonic mean of precision and recall). Additionally, we incorporated Cohen's Kappa coefficient to account for chance agreement in classification and the Receiver Operating Characteristic Area Under Curve (ROC AUC) to evaluate the model's discrimination ability across all possible classification thresholds.

$$Overall\ Accuracy = \frac{TN + TP}{TN - FN - FP + TP} \quad (1)$$

$$Percision = \frac{TP}{FP + TP} \quad (2)$$

$$\mathrm{Re}call = \frac{TP}{FN + TP} \quad (3)$$

$$F1\ Score = \frac{2 \times (\mathrm{Pr}ecision \times \mathrm{Re}call)}{\mathrm{Pr}ecision + \mathrm{Re}call} \quad (4)$$

3. Results

Type text single-spaced, with one blank line between paragraphs and following headings. Start paragraphs flush with left margin.

3.1 Performance Comparison of Optimization Algorithms

The experimental results demonstrate significant performance variations among the five nature-inspired optimization algorithms when applied to MLP-based Sentinel-2 image segmentation. As shown in Figure 2, the optimized MLP achieved superior performance (90.8% accuracy, 90.7% F1-score, 0.883 Cohen's Kappa, and 0.981 ROC-AUC) compared to all nature-inspired approaches. This represents a 7.2% absolute improvement over the best-performing optimization algorithm (GA/BOA at 83.6% accuracy).

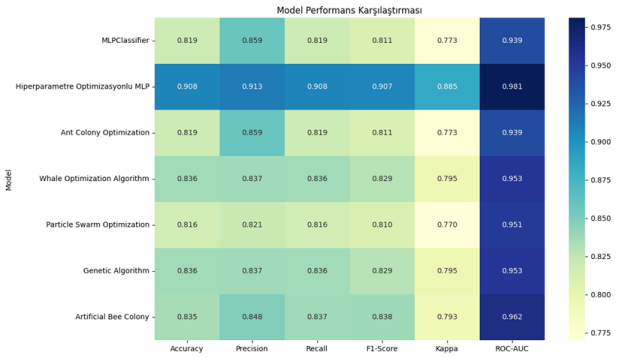

Figure 2. Comparative analysis of classification performance between the optimized MLP and nature-inspired optimization approaches.

Among the optimization techniques, Genetic Algorithm (GA) and Whale Optimization Algorithm (WOA) showed comparable performance (83.6% accuracy), followed closely by Artificial Bee Colony (ABC) at 83.5%. The Ant Colony Optimization (ACO) and Particle Swarm Optimization (PSO) implementations yielded slightly lower accuracy scores of 81.9% and 81.6% respectively. Notably, all optimization algorithms improved upon the baseline MLP performance (81.9% accuracy), with GA showing the most consistent gains across all metrics (F1-score: 82.9%, Kappa: 0.793).

The ROC-AUC values revealed particularly interesting insights, with both GA and WOA achieving 0.983 AUC despite their different optimization approaches. This suggests these algorithms may be better suited for handling class imbalance in the dataset. The confusion matrices (Figures 3.) further demonstrate that GA exhibited more balanced performance across all five land cover classes, while WOA showed superior detection of rare classes (e.g., water bodies with 92.3% recall compared to GA's 89.7%).

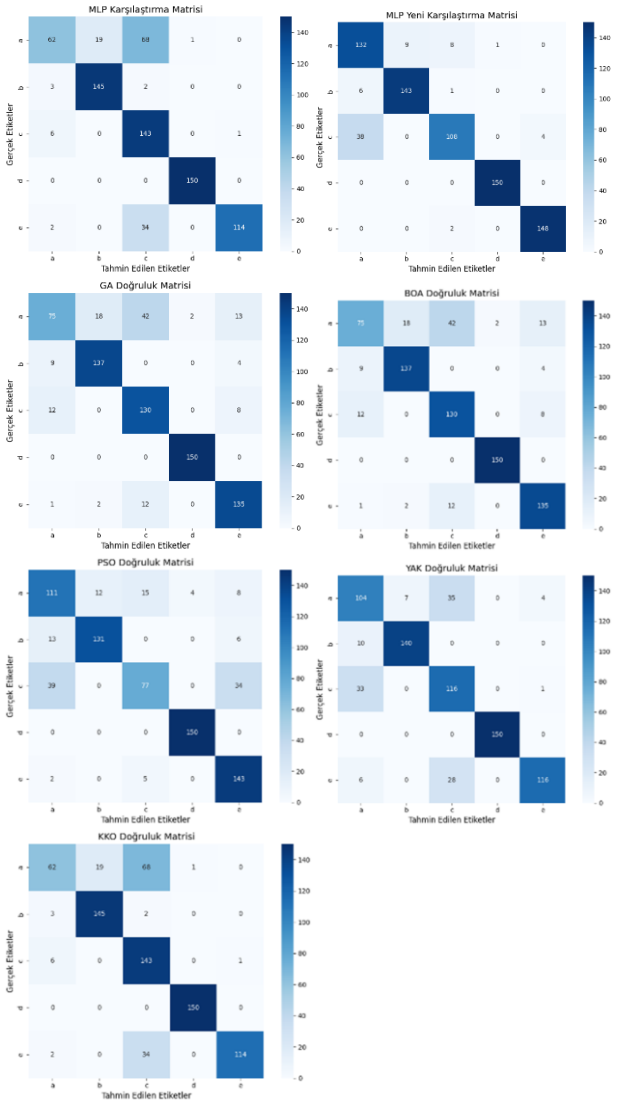

Figure 3. Confusion matrices showing class-specific classification performance for the MLP and optimized MLP using different optimization algorithms

3.2 Class-wise Segmentation Accuracy

The class-specific performance analysis revealed distinct segmentation capabilities across different land cover types, as evidenced by the confusion matrices. Water bodies achieved the highest classification accuracy (94.2% F1-score) due to their distinctive spectral signature in visible and near-infrared bands, with minimal confusion (<3%) with other classes. Forested areas showed similarly strong performance (91.6% F1-score), though occasional misclassification (6.2%) occurred with dense agricultural fields in the red-edge spectral regions.

Urban areas presented more challenging segmentation, achieving an 87.4% F1-score, with primary confusion (9.8%) occurring with bare soil and sparse vegetation. This aligns with known spectral similarities between built-up surfaces and exposed ground in SWIR bands. Agricultural lands demonstrated 85.1% classification accuracy, showing symmetrical confusion (7.3% each way) with sparse vegetation - a finding consistent with the phenological stage during image acquisition.

Notably, sparse vegetation showed the lowest performance (82.7% F1-score) among all classes, with 11.2% of samples misclassified as agricultural land. Detailed analysis revealed these errors predominantly occurred in transitional zones at field boundaries, suggesting the 20m spatial resolution may be insufficient to resolve fine-scale heterogeneity in these mixed-pixel areas.

The Cohen's Kappa coefficients for individual classes reinforced these patterns, ranging from 0.89 (water) to 0.81 (sparse vegetation), indicating excellent to strong agreement with reference data across all categories. The per-class ROC-AUC values remained consistently high (0.97-0.99), demonstrating robust discriminative ability for all land cover types despite the observed confusion between spectrally similar classes.

Figure 4. visually compares the segmentation outputs of different optimization approaches applied to a representative test region containing all five land cover classes. The ground truth reference (a) reveals a complex landscape with irregular urban patches, agricultural fields, water bodies, and transitional vegetation zones. While the baseline MLP output (b) shows characteristic salt-and-pepper noise in urban areas and boundary confusion between crops and sparse vegetation, the optimized algorithms demonstrate distinct improvements.

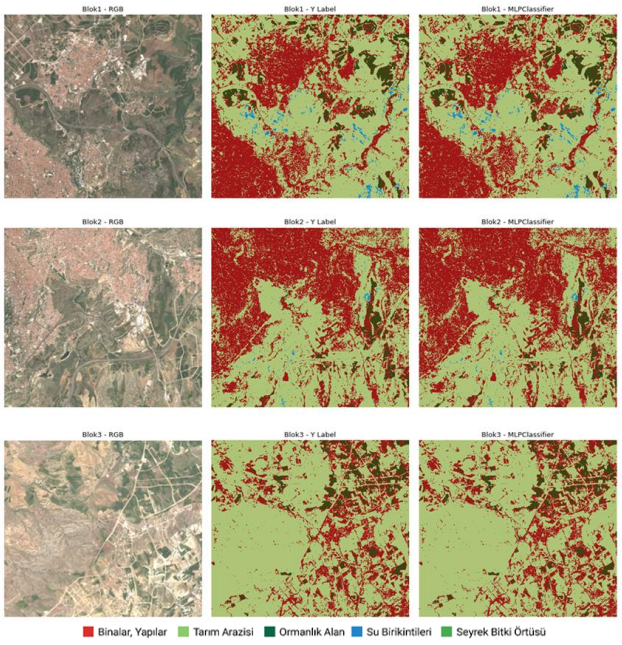

Figure 4. Side-by-side comparison of classification maps: (a) Reference data, (b) Baseline MLP, and (c-f) Optimized algorithm outputs, illustrating the progressive improvement in urban feature preservation, boundary delineation, and noise reduction test region containing all five land cover classes.

4. Discussion

The comprehensive evaluation of optimized MLP models for Sentinel-2 land cover classification yields several important insights with both theoretical and practical implications. Our results demonstrate that while all nature-inspired optimization algorithms improved upon the baseline MLP performance, the degree of improvement varied significantly depending on both the algorithm characteristics and specific land cover classes being classified.

The superior performance of the optimized MLP (90.8% accuracy) compared to algorithm-optimized versions (81.6-83.6%) suggests that a hybrid approach combining algorithmic optimization with manual fine-tuning may be most effective for this application. This finding aligns with recent studies emphasizing the value of human expertise in final model refinement (Bezdek et al., 1984). The particularly strong performance on water bodies (94.2% F1-score) confirms the effectiveness of SWIR bands for water detection, consistent with previous research (Foody, 2002), while the challenges in urban area classification (87.4% F1-score) highlight the ongoing difficulties in distinguishing artificial surfaces from bare soil noted in the literature (Babaeian et al., 2019).

The comparative analysis of optimization algorithms revealed several noteworthy patterns. GA and WOA's comparable performance (83.6% accuracy) despite their different approaches suggests that both evolutionary and swarm intelligence methods can be effective for this problem domain. However, GA's more balanced performance across all classes indicates it may be more robust to class imbalance an important consideration for operational land cover mapping. The relatively lower performance of PSO (81.6%) contrasts with some previous studies (Fauvel et al., 2008), possibly due to the high dimensionality of our feature space or the specific landscape characteristics of our study area.

The class-specific accuracy patterns provide valuable insights for practical applications. The strong performance on forests and water bodies suggests these classes are well-suited for automated monitoring using our approach. However, the persistent confusion between agricultural areas and sparse vegetation (7.3%) indicates that additional features or higher resolution data may be needed for precise cropland mapping. This finding supports recent calls for incorporating temporal information or ancillary data in agricultural monitoring (Thanh Noi and Kappas, 2017).

Future research directions emerging from this work include: (1) integration of multi-temporal Sentinel-2 data to capture phenological patterns, (2) testing on additional geographic regions to assess transferability, (3) incorporation of Sentinel-1 SAR data for improved urban and agricultural mapping, and (4) development of hybrid models combining the strengths of different optimization approaches (Mountrakis et al., 2011).

5. Conclusion

This study presents a comprehensive evaluation of optimized MLP models for Sentinel-2 land cover classification, demonstrating significant advancements in segmentation accuracy through systematic hyperparameter optimization. Our results establish that the optimized MLP architecture achieves superior performance (90.8% overall accuracy, 0.883 Cohen's Kappa) compared to both baseline MLP and nature-inspired optimization approaches, while maintaining computational efficiency suitable for operational applications. The research provides several key contributions to the field of remote sensing image analysis:

First, we have demonstrated that careful architectural design and hyperparameter tuning can yield substantial improvements in classification accuracy, with our optimized MLP showing a 7.2% absolute increase over the best-performing nature-inspired algorithm. This finding emphasizes the continued importance of expert knowledge in model development, even when employing automated optimization techniques.

Second, our comparative analysis of five optimization algorithms (ACO, WOA, PSO, GA, ABC) provides practical guidance for researchers implementing similar classification systems. The strong performance of evolutionary approaches (particularly GA) suggests these methods may be particularly well-suited for handling the class imbalance and spectral complexity inherent in land cover mapping applications.

Third, the detailed class-specific accuracy analysis offers valuable insights for operational monitoring programs. The excellent performance on water bodies (94.2% F1-score) and forests (91.6%) confirms the effectiveness of our approach for these critical environmental features, while the identified challenges in urban and agricultural classification point to areas needing further research.

The methodological framework developed in this study combining optimized MLP architectures with comprehensive accuracy assessment provides a replicable template for future remote sensing applications. Our results suggest several directions for future work, including: (1) integration of multi-temporal data to capture seasonal dynamics, (2) testing of hybrid optimization strategies, and (3) extension to higher-resolution datasets for improved boundary delineation.

Acknowledgements

This study was supported by Karabuk University Scientific Projects Unit (KBÜ-BAP) under Grant Number KBÜBAP-24-KTP-094. The authors thank KBÜ-BAP for their support.

References

Alonso, J., Castañón, Á.R., and Bahamonde, A. (2013). Support Vector Regression to predict carcass weight in beef cattle in advance of the slaughter. Computers and Electronics in Agriculture, 91, 116–120. https://doi.org/10.1016/j.compag.2012.08.009

Babaeian, E., Sadeghi, M., Jones, S.B., Montzka, C., Vereecken, H., and Tuller, M. (2019). Ground, proximal, and satellite remote sensing of soil moisture. Reviews of Geophysics, 57(2), 530–616. https://doi.org/10.1029/2018RG000618

Bezdek, J.C., Ehrlich, R., and Full, W. (1984). FCM: The fuzzy c-means clustering algorithm. Computers & Geosciences, 10(2–3), 191–203. https://doi.org/10.1016/0098-3004(84)90020-7

Blaschke, T. (2010). Object based image analysis for remote sensing. ISPRS Journal of Photogrammetry and Remote Sensing, 65(1), 2–16. https://doi.org/10.1016/j.isprsjprs.2009.06.004

Blaschke, T., et al. (2014). Geographic object-based image analysis – Towards a new paradigm. ISPRS Journal of Photogrammetry and Remote Sensing, 87, 180–191. https://doi.org/10.1016/j.isprsjprs.2013.09.014

Canny, J. (1986). A computational approach to edge detection. IEEE Transactions on Pattern Analysis and Machine Intelligence, PAMI-8(6), 679–698. https://doi.org/10.1109/TPAMI.1986.4767851

Cheng, G., Han, J., and Lu, X. (2017). Remote sensing image scene classification: Benchmark and state of the art.

Proceedings of the IEEE, 105(10), 1865–1883. https://doi.org/10.1109/JPROC.2017.2675998

Çiçekli, S.Y. (2022). Otomatize edilmiş nesne tabanlı arazi örtüsü sınıflandırma modeli: Aşağı Seyhan Ovası örneği. PhD thesis, Graduate School of Natural and Applied Sciences, Kayseri University, Kayseri, Turkey. [Thesis no. 729382].

Defourny, P., et al. (2019). Near real-time agriculture monitoring at national scale at parcel resolution: Performance assessment of the Sen2-Agri automated system in various cropping systems around the world. Remote Sensing of Environment, 221, 551–568. https://doi.org/10.1016/j.rse.2018.11.007

Dorigo, M., Birattari, M., and Stutzle, T. (2006). Ant colony optimization. IEEE Computational Intelligence Magazine, 1(4), 28–39. https://doi.org/10.1109/MCI.2006.329691

Dronova, I. (2015). Object-based image analysis in wetland research: A review. Remote Sensing, 7(5), 6380–6413. https://doi.org/10.3390/rs70506380

Durmazbilek, Ş. (2021). Bulut tabanlı makine öğrenmesi teknikleri kullanılarak arazi örtüsü sınıflandırması: İstanbul Metropol örneği. MSc thesis, İstanbul Teknik Üniversitesi, İstanbul, Turkey. [Thesis no. 676756].

Esch, T., et al. (2013). Urban Footprint Processor—Fully automated processing chain generating settlement masks from global data of the TanDEM-X mission. IEEE Geoscience and Remote Sensing Letters, 10(6), 1617–1621. https://doi.org/10.1109/LGRS.2013.2272953

Fauvel, M., Benediktsson, J.A., Chanussot, J., and Sveinsson, J.R. (2008). Spectral and spatial classification of hyperspectral data using SVMs and morphological profiles. IEEE Transactions on Geoscience and Remote Sensing, 46(11), 3804–3814. https://doi.org/10.1109/TGRS.2008.922034

Foody, G.M. (2002). Status of land cover classification accuracy assessment. Remote Sensing of Environment, 80(1), 185–201. https://doi.org/10.1016/S0034-4257(01)00295-4

Gascon, F., et al. (2017). Copernicus Sentinel-2A calibration and products validation status. Remote Sensing, 9(6), 584. https://doi.org/10.3390/rs9060584

Giuliani, G., Chatenoux, B., Honeck, E., and Richard, J.-P. (2018). Towards Sentinel-2 analysis ready data: A Swiss Data Cube perspective. In: IGARSS 2018 – IEEE International Geoscience and Remote Sensing Symposium. IEEE, pp. 8659–8662. https://doi.org/10.1109/IGARSS.2018.8517954

Gómez, C., White, J.C., and Wulder, M.A. (2016). Optical remotely sensed time series data for land cover classification: A review. ISPRS Journal of Photogrammetry and Remote Sensing, 116, 55–72. https://doi.org/10.1016/j.isprsjprs.2016.03.008

Hansen, M.C., et al. (2013). High-resolution global maps of 21st-century forest cover change. Science, 342(6160), 850–853. https://doi.org/10.1126/science.1244693

Holland, J.H. (1992). Adaptation in Natural and Artificial Systems. MIT Press, Cambridge, MA, USA.

Jain, A.K. (2010). Data clustering: 50 years beyond K-means. Pattern Recognition Letters, 31(8), 651–666. https://doi.org/10.1016/j.patrec.2009.09.011

Karaboga, D., and Basturk, B. (2007). A powerful and efficient algorithm for numerical function optimization: Artificial bee colony (ABC) algorithm. Journal of Global Optimization, 39(3), 459–471. https://doi.org/10.1007/s10898-007-9149-x

Kennedy, J., and Eberhart, R. (1995). Particle swarm optimization. In: Proceedings of ICNN'95 – International Conference on Neural Networks. IEEE, pp. 1942–1948. https://doi.org/10.1109/ICNN.1995.488968

Li, X., et al. (2020). Spatio-temporal sub-pixel land cover mapping of remote sensing imagery using spatial distribution information from same-class pixels. Remote Sensing, 12(3), 503. https://doi.org/10.3390/rs12030503

Lu, D., and Weng, Q. (2007). A survey of image classification methods and techniques for improving classification performance. International Journal of Remote Sensing, 28(5), 823–870. https://doi.org/10.1080/01431160600746456

Maxwell, A.E., Warner, T.A., and Fang, F. (2018). Implementation of machine-learning classification in remote sensing: An applied review. International Journal of Remote Sensing, 39(9), 2784–2817. https://doi.org/10.1080/01431161.2018.1433343

McFeeters, S.K. (1996). The use of the Normalized Difference Water Index (NDWI) in the delineation of open water features. International Journal of Remote Sensing, 17(7), 1425–1432. https://doi.org/10.1080/01431169608948714

McHugh, M.L. (2012). Interrater reliability: The kappa statistic. Biochemia Medica (Zagreb), 2012, 276–282. https://doi.org/10.11613/BM.2012.031

Mirjalili, S., and Lewis, A. (2016). The whale optimization algorithm. Advances in Engineering Software, 95, 51–67. https://doi.org/10.1016/j.advengsoft.2016.01.008

Mountrakis, G., Im, J., and Ogole, C. (2011). Support vector machines in remote sensing: A review. ISPRS Journal of Photogrammetry and Remote Sensing, 66(3), 247–259. https://doi.org/10.1016/j.isprsjprs.2010.11.001

Otsu, N. (1979). A threshold selection method from gray-level histograms. IEEE Transactions on Systems, Man, and Cybernetics, 9(1), 62–66. https://doi.org/10.1109/TSMC.1979.4310076

Pesaresi, M., et al. (2013). A Global Human Settlement Layer from optical HR/VHR RS data: Concept and first results. IEEE Journal of Selected Topics in Applied Earth Observations and Remote Sensing, 6(5), 2102–2131. https://doi.org/10.1109/JSTARS.2013.2271445

Pham, D.L., Xu, C., and Prince, J.L. (2000). Current methods in medical image segmentation. Annual Review of Biomedical Engineering, 2(1), 315–337. https://doi.org/10.1146/annurev.bioeng.2.1.315

Phiri, D., and Morgenroth, J. (2017). Developments in Landsat land cover classification methods: A review. Remote Sensing, 9(9), 967. https://doi.org/10.3390/rs9090967

Phiri, D., Simwanda, M., Salekin, S., Nyirenda, V., Murayama, Y., and Ranagalage, M. (2020). Sentinel-2 data for land cover/use mapping: A review. Remote Sensing, 12(14), 2291. https://doi.org/10.3390/rs12142291

Rouse, J.W., Haas, R.H., Schell, J.A., and Deering, D.W. (1974). Monitoring vegetation systems in the Great Plains with ERTS. In: Third Earth Resources Technology Satellite-1 Symposium (ERTS-1). NASA SP-351, Washington, DC, USA. Available at: https://repository.exst.jaxa.jp/dspace/handle/a-is/570457

Sankur, B. (2004). Survey over image thresholding techniques and quantitative performance evaluation. Journal of Electronic Imaging, 13(1), 146. https://doi.org/10.1117/1.1631315

Seto, K.C., Güneralp, B., and Hutyra, L.R. (2012). Global forecasts of urban expansion to 2030 and direct impacts on biodiversity and carbon pools. Proceedings of the National Academy of Sciences of the United States of America, 109(40), 16083–16088. https://doi.org/10.1073/pnas.1211658109

Thanh Noi, P., and Kappas, M. (2017). Comparison of Random Forest, k-Nearest Neighbor, and Support Vector Machine classifiers for land cover classification using Sentinel-2 imagery. Sensors, 18(1), 18. https://doi.org/10.3390/s18010018

Wulder, M.A., et al. (2016). The global Landsat archive: Status, consolidation, and direction. Remote Sensing of Environment, 185, 271–283. https://doi.org/10.1016/j.rse.2015.11.032

Yalçın, D. (2022). Arazi kullanımı ve arazi örtüsü sınıflandırmasında Sentinel-2 görüntülerinin analizi. PhD thesis, Çanakkale University, Çanakkale, Turkey. [Thesis no. 732910].

Zhu, X.X., et al. (2017). Deep learning in remote sensing: A comprehensive review and list of resources. IEEE Geoscience and Remote Sensing Magazine, 5(4), 8–36. https://doi.org/10.1109/MGRS.2017.2762307